

Aluminium diffusion in decagonal quasicrystals

S. Hocker and F. Gähler

*Institut für Theoretische und Angewandte Physik,
Universität Stuttgart, D-70550 Stuttgart, Germany*

Aluminium is the majority element in many quasicrystals and expected to be the most mobile element, but its diffusion properties are hardly accessible to experiment. Here we investigate aluminium diffusion in decagonal Al-Ni-Co and Al-Cu-Co quasicrystals by molecular dynamics simulations, using classical effective pair potentials. Above two thirds of the melting temperature, strong aluminium diffusion is observed. The diffusion constant is measured as a function of temperature and pressure, from which the activation enthalpies and activation volumes are determined. As there are no vacancies in the samples, the diffusion, which is anisotropic, must use a direct mechanism. The high mobility of aluminium is also relevant for structure determination, and will contribute to diffuse scattering. The qualitative behaviour of the dynamics is confirmed by ab-initio simulations.

PACS numbers: 66.30.Fq,61.44.Br

Understanding atomic diffusion in quasicrystals is essential for comprehending many physical processes in these complex alloys. Diffusion is required for the formation of the equilibrium phase during high temperature annealing and for the motion of dislocations and other defects. Unfortunately, due to the lack of suitable radiotracers, it is very hard to measure Al diffusion experimentally. No such studies have been presented so far. Molecular dynamics (MD) simulations can here complement the experimental methods. In this Letter, we present MD simulations which allow us not only to determine the microscopic dynamics of the Al atoms, but also to measure the macroscopic diffusion constant as a function of temperature and pressure. MD simulations thus provide an excellent tool for the study of atomic dynamics both at the microscopic and the macroscopic level.

The reliability of MD simulations crucially depends on the quality of the potentials. Direct numerical diffusion measurements are feasible only with classical effective potentials. Quantum-mechanical simulations are limited to a few hundred atoms, which can neither provide enough statistics nor model the aperiodic nature of quasicrystals. Here, we use the Al-TM (transition metal) potentials of Moriarty and Widom [1, 2], derived from density functional theory. The restriction to pair potentials is compensated by an additional, empirical pair potential correction for the TM-TM interactions (except for Cu-Cu), which is fitted to an ab-initio simulation of a small quasicrystal approximant [3]. The so corrected effective pair potentials are smoothly truncated at a radius of about 7.5\AA . A characteristic feature of the potential functions is their long range Friedel oscillations. The Moriarty-Widom potentials turn out to be clearly superior to previous potentials of Phillips et al. [4] employed in earlier simulations of decagonal quasicrystals [5, 6]. All simulations were carried out with the code IMD [7] developed at our institute.

We consider four different model structures, three for

decagonal Al-Ni-Co, and one for decagonal Al-Cu-Co. All four models essentially consist of an alternating stacking of two different layers, which are decorations of the same hexagon-boat-star (HBS) tiling, resulting in a period of about 4\AA . All models share most of the atom positions; the difference is mainly in the chemistry of the decoration. The first two decorations for Al-Ni-Co, called Ni-rich ($\text{Al}_{70}\text{Ni}_{21}\text{Co}_9$) and Co-rich ($\text{Al}_{72}\text{Ni}_{17}\text{Co}_{11}$), have been derived in [8] by optimizing the model structure with respect to the Moriarty-Widom potentials. We use slightly modified variants determined in relaxation simulations [9], where it was found that the two innermost Al atoms in the star tiles prefer different positions, and also break the 4\AA periodicity locally to an 8\AA periodicity (see also [10]). The modified Ni-rich decoration is shown in Fig. 1. The Co-rich decoration is obtained from it by replacing certain Ni-Ni pairs in hexagon tiles by Co-Al pairs, which is energetically favourable [8]. The third decoration for Al-Ni-Co ($\text{Al}_{72}\text{Ni}_{20}\text{Co}_8$), called Abe decoration, is inspired by the cluster model of Abe et al. [11]. As it originally was given only for one cluster, it had to be extrapolated in order to define a decoration also for approximants, which are not completely covered by clusters. To a large extent, the Ni-Co decoration of the Abe model is reversed with respect to the Ni-rich decoration. The Co atoms inside supertiles are replaced by Ni atoms, and Ni-Ni pairs on supertile edges are replaced by Ni-Co pairs, where one of the sites of such a pair may also be empty [11]. The Al decoration is mostly the same as for the Ni-rich decoration, except that the two innermost Al atoms in star tiles are missing. The Ni-Co decoration of the Abe model is not supported by total energy calculations [8, 10], but allows to determine whether it is the chemical or the geometrical environment which determines the Al mobility. Finally, for decagonal Al-Cu-Co we use a variant [12] of the decoration proposed by Cockayne et al. [13], with a composition of $\text{Al}_{70}\text{Cu}_{10}\text{Co}_{20}$. It is obtained from the Ni-rich decoration by replacing each Ni-Ni pair on supertile edges by a Cu-Co pair.

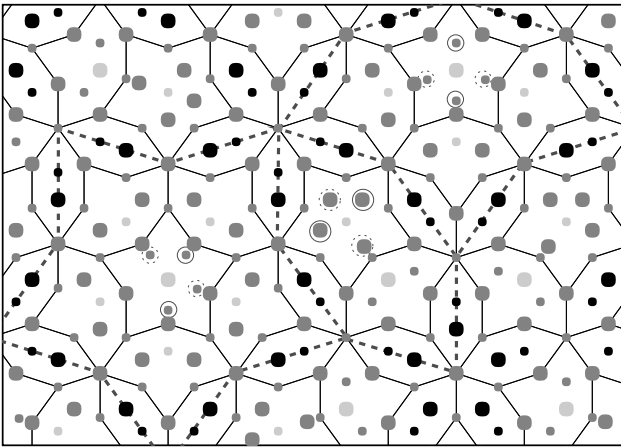


FIG. 1: Ni-rich decoration after relaxation. The positions of the marked atoms differ from the original decoration [8]. Small (large) dots indicate atoms in upper (lower) layer. Al: dark grey, Ni: black, Co: light grey. Dashed lines mark superlattices. Encircled atoms occur only in every second double layer, those with solid circles in one half of the double layers, those with dashed circles in the other half.

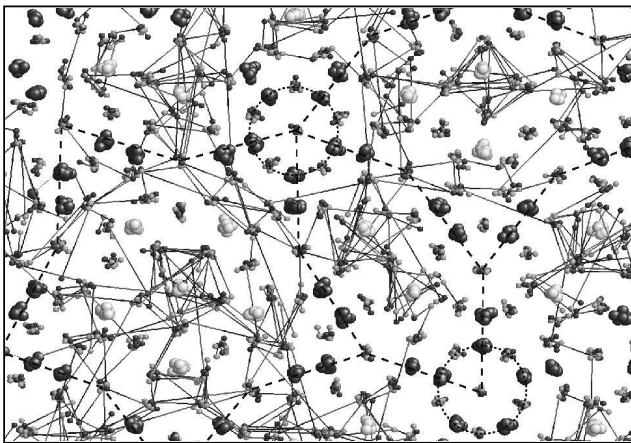


FIG. 2: Al motion at $T = 0.9T_m$ in the Ni-rich sample. Dark grey, large: Ni; light grey, large: Co; dark grey, small: Al initial positions; light grey, small: Al positions after 100ps. Initial and final Al positions are connected. Supertiles and stable clusters are marked.

All samples had about 3360 atoms ($52\text{\AA} \times 38\text{\AA} \times 25\text{\AA}$, six double layers). In order to check the correctness of the energy scale of the potentials, the melting temperatures T_m of the different samples were first determined by slowly heating the samples at constant pressure. The Al-Ni-Co systems melted at about 1250 K (Ni-rich), 1170 K (Co-rich), and 1115 K (Abe model), which is reasonably close to the experimental melting temperature of the basic Ni-rich phase of about 1200 K [15]. The Al-Cu-Co sample also melted at reasonable 1183 K.

The remaining simulations were carried out at constant temperature and volume, using a leap-frog integrator with Nosé-Hoover thermostat [14]. The time step was

1fs. At each temperature, the sample was suitably scaled to adjust the pressure, and then equilibrated over a few 10^4 time steps. Each diffusion measurement then ran over two million time steps (2ns). Apart from the initial relaxations described in Fig. 1 and in [9], which may locally break the 4\AA periodicity, all samples remained essentially stable up to the melting temperature. Above $0.6T_m$ significant diffusion of Al is observed (Fig. 2), which does not destroy the overall structure, however. Time-averaged atom density maps (Fig. 3) show that all TM sites and some Al sites remain very sharp over the 2ns simulation period, whereas most of the other Al sites are smeared out in certain directions, but are still stable and well identifiable. The most mobile Al atoms are the ones near the Co sites of the Ni-rich decoration. A comparison with the other samples shows that this mobility is not so much due to the Co atoms, but rather due to the geometrical environment of the Co sites. In the Abe model, where the corresponding sites are occupied by Ni, the same Al atoms show an enhanced mobility. Not all Al atoms become mobile, however. In Figs. 2 and 3 one can see stable, columnar clusters of 5 Al and 5 Ni atoms per period, whose Al atoms do not move beyond local vibrations around their equilibrium positions. The mobile Al atoms are sufficiently frequent (75-80% of all Al atoms) and their sites sufficiently close to each other, that long range diffusion is possible. The mobility of TM atoms is much smaller, so that within the accessible time scales it is not feasible to measure their diffusivity by MD.

The atom density maps (Fig. 3) reveal that the ba-

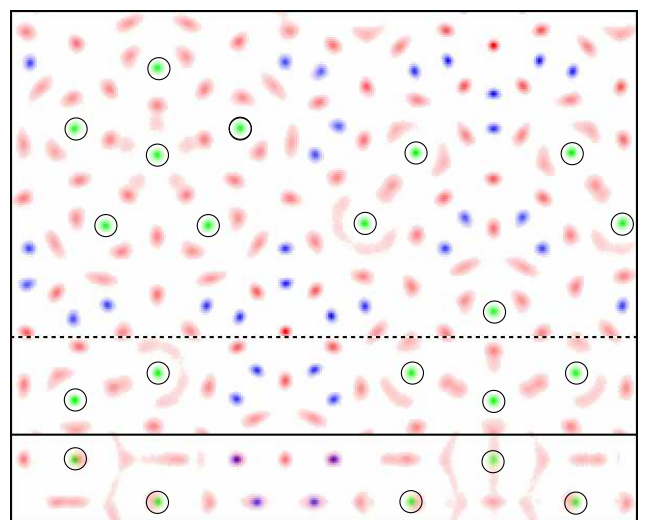


FIG. 3: (Color online) Atom density map of Ni-rich Al-Ni-Co, averaged over 2ns. Above the solid line, the projection on the xy -plane is shown. The part below the dotted line is shown again in the bottom, but projected on the xz -plane. Co positions (online: green) are marked with circles; Ni positions (online: blue) appear as sharp, almost black dots, whereas Al positions (online: red) are grayish.

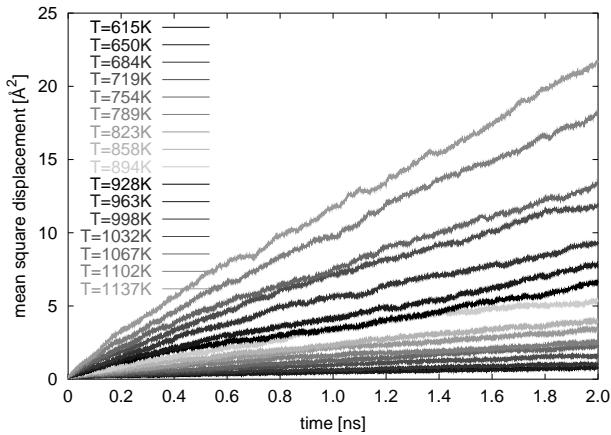


FIG. 4: Mean square displacement of Al in the Co-rich sample as a function of time, at different temperatures. Shown are the displacements in the x-direction.

nana shaped Al sites near the TM sites inside supertile hexagons are smeared out only horizontally, whereas the central dot between these TM sites is actually a zig-zag shaped distribution continuous along the z -axis, having three maxima per two periods [10]. The potential valleys seen by most of the mobile Al atoms are shallow only in one direction, but enhanced Al mobility can occur in all directions. The diffusion in z -direction occurs mostly along the few continuous channels, where Al atoms are extremely mobile. On the other hand, many more atoms participate in the diffusion in the xy -plane, but move less quickly on average. Al atoms can also enter and leave the fast diffusion channels. The smeared-out Al sites certainly have to be taken into account in the interpretation of diffraction data, and possibly can explain some of the diffuse scattering intrinsic in these quasicrystals [16].

The vacancies initially present in the Abe model are not stable. The available space is immediately filled by Al atoms, which are redistributed such that the vacancies are smeared out over many Al sites, and are no longer identifiable. Due to the deep nearest neighbour Al-TM minima and next nearest neighbour TM-TM minima of the potentials [3], the quasicrystal structure can be regarded as a stable TM backbone held together by Al glue. Apart from the hard core, Al-Al interactions are very weak, so that the precise distribution of Al between the TM atoms is only of minor importance.

To determine the Al diffusion quantitatively, we have measured the mean square displacement (MSQD) of Al as a function of time. From the slope of these curves, the diffusion constant is extracted. This is first done for different temperatures at pressure zero, and then with varying pressure at a fixed temperature close to the melting point. As illustration, some of the MSQD curves for the Co-rich sample are shown in Fig. 4 (see also [9, 17]). The MSQD curves were then fitted to the usual Arrhenius law

TABLE I: Activation enthalpies, activation volumes, and pre-exponential factors for Al diffusion. Ω is the average atomic volume.

Sample	Ni-rich	Co-rich	Abe	Al-Cu-Co
ΔH_{xy} [eV]	0.89	0.41	0.34	0.75
ΔH_z [eV]	0.64	0.38	0.35	0.86
ΔV_{xy} [Ω]	0.25	0.13	0.17	0.48
ΔV_z [Ω]	0.38	0.087	0.17	0.27
D_{0xy} [m^2/s]	$1.8 \cdot 10^{-7}$	$2.6 \cdot 10^{-9}$	$4.6 \cdot 10^{-9}$	$9.0 \cdot 10^{-8}$
D_{0z} [m^2/s]	$6.3 \cdot 10^{-8}$	$9.7 \cdot 10^{-9}$	$1.8 \cdot 10^{-8}$	$1.5 \cdot 10^{-6}$

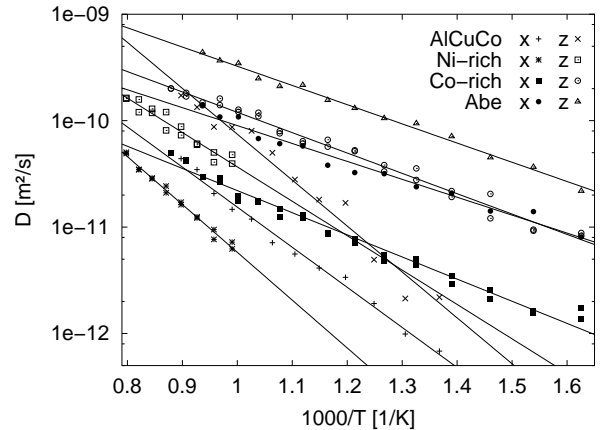


FIG. 5: Arrhenius plots for Al diffusion.

for the diffusion constant D ,

$$D = D_0 e^{-\left(\frac{\Delta H + p\Delta V}{k_B T}\right)} \quad (1)$$

from which the activation enthalpy ΔH , activation volume ΔV , and pre-exponential factors D_0 could be determined, separately for the x -, the y -, and the z -directions. The values are given in Table I, and the fit to the Arrhenius law is shown in Fig. 5. The diffusion is anisotropic, by a factor 2-3 faster in the periodic direction. The activation enthalpies obtained are rather low, compared with the value for vacancy diffusion in FCC Al (1.26 eV) [18]. However, due to the short time scales in the simulation, the concentration of vacancies or other diffusion vehicles is not in equilibrium, so that only the migration enthalpy is measured [19], not the full activation enthalpy. The values we obtain compare well with the vacancy migration enthalpy of FCC Al (0.61 eV) [18]. The same problem occurs with the activation volumes, which are in the range of 10-50% of the average atomic volume, Ω . These should be interpreted as migration volumes, not full activation volumes. The values given in Table I are therefore compatible with vacancy diffusion as observed for other diffusers [20]. Nevertheless, as our samples did not contain vacancies (except for the Abe model), the diffusion seen here must use a different, direct mechanism,

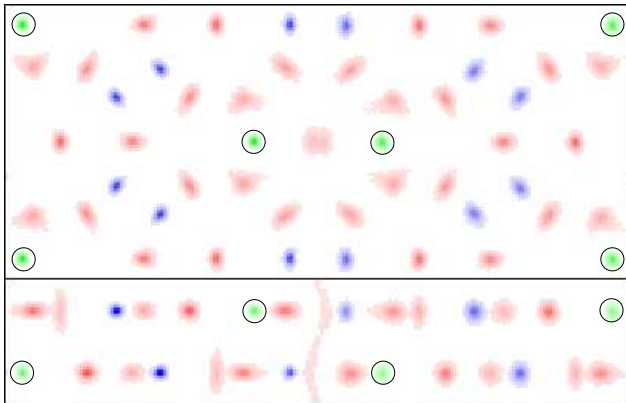


FIG. 6: (Color online) Atom density distribution for classical MD (left half) and ab-initio MD (right half), averaged over 100ps, for one supertile hexagon (25 atoms). Shown is the projection on the xy -plane (top) and on the xz -plane (bottom). Co positions (online: green) are marked with circles; Ni positions (online: blue) appear as sharp, almost black dots, whereas Al positions (online: red) are grayish.

and cannot be vacancy mediated. Given the stability of the TM sites, it seems also difficult to interpret it as being phason induced [21].

The quantitative correctness of our results crucially depends on the quality of the potentials, which have been tested mainly for ground state type structures [2]. It is unclear whether the energetics of the diffusion processes at high temperatures are described correctly, so that there is some uncertainty in the numerical values given in Table I. However, the diffusion constant of Zn in decagonal Al-Ni-Co, which is believed to behave similarly to Al, is roughly comparable [22] when extrapolated to the high temperatures considered here, which adds some confidence to our results.

As a further check, we have simulated a small sample of one supertile hexagon (25 atoms) with both ab-initio MD and classical MD, under precisely the same conditions. The ab-initio simulation was carried out with VASP [23] using the PAW method [24]. Since ab-initio MD is much slower than classical MD, these simulations could span a time interval of only 100ps, so that it is not possible to directly measure the diffusion constant. The atom density maps obtained in these simulations are very similar, however (Fig. 6). In particular, all Al sites are smeared out in exactly the same way. There is only one systematic difference: in ab-initio MD the atom distributions appear smoother than in classical MD, implying that the potential is slightly softer in a quantum-mechanical treatment.

Our simulations could not confirm the experimental evidence for vacancy mediated diffusion [20]. Vacancies initially present in the Abe model have even been dissolved. A proper simulation of systems with vacancies would probably require many body potentials, like embedded-atom method (EAM) potentials [25]. The latter include effects of the conduction electrons, and are

better suited in situations of low or varying coordination. Simple pair potentials are well known for not being able to describe vacancies adequately. Unfortunately, EAM potentials are presently not available for such complicated structures.

The authors would like to thank Mike Widom and Marek Mihalkovič, who kindly provided the potentials and the initial model structures.

-
- [1] J.A. Moriarty and M. Widom, *Phys. Rev. B* **56**, 7905 (1997).
 - [2] M. Widom, I. Al-Lehyani, and J.A. Moriarty, *Phys. Rev. B* **62**, 3648 (2000).
 - [3] I. Al-Lehyani, M. Widom, Y. Wang, N. Moghadam, G.M. Stocks, and J.A. Moriarty, *Phys. Rev. B* **64**, 075109 (2001).
 - [4] R. Phillips, J. Zou, A.E. Carlsson, and M. Widom, *Phys. Rev. B* **49**, 9322 (1994).
 - [5] D. Bunz, G. Zeger, J. Roth, M. Hohl, and H.-R. Trebin, *Mater. Sci. Eng. A* **296**, 675 (2000).
 - [6] M. Mihalkovic, H. Elhor, and J.-B. Suck, *Phys. Rev. B* **63**, 214301 (2001).
 - [7] J. Stadler, R. Mikulla, and H.-R. Trebin, *Int. J. Mod. Phys. C* **8**, 1131 (1997).
<http://www.itap.physik.uni-stuttgart.de/~imd/>
 - [8] M. Mihalkovic, I. Al-Lehyani, E. Cockayne, C.L. Henley, N. Moghadam, J.A. Moriarty, Y. Wang, and M. Widom, *Phys. Rev. B* **65**, 104205 (2001).
 - [9] F. Gähler and S. Hocker, *J. Non-Cryst. Solids* **334–335**, 308 (2004). Note an error of time scale in this article: simulations are over 2ns, not 20ns.
 - [10] C.L. Henley, M. Mihalkovic, and M. Widom, *J. All. Comp.* **342**, 221 (2002).
 - [11] E. Abe, K. Saitoh, H. Takakura, A.P. Tsai, P.J. Steinhart, and H.-C. Jeong, *Phys. Rev. Lett.* **84**, 4609 (2000).
 - [12] I. Al-Lehyani and M. Widom, *Phys. Rev. B* **67**, 014204 (2003).
 - [13] E. Cockayne and M. Widom, *Phys. Rev. Lett.* **81**, 598 (1998).
 - [14] M. P. Allen and D. J. Tildesley, *Computer Simulation of Liquids* (Clarendon Press, Oxford, 1992).
 - [15] S. Ritsch, C. Beeli, H.-U. Nissen, T. Gödecke, M. Scheffer, and R. Lück, *Phil. Mag. Lett.* **78**, 67 (1998).
 - [16] F. Frey and E. Weidner, *Z. Kristallogr.* **218**, 160 (2003).
 - [17] F. Gähler and S. Hocker, *Ferroelectrics* **308**, 167 (2004).
 - [18] P. Erhart, in *Landolt-Börnstein, New Series III, Vol. 25*, edited by H. Ullmaier, (Springer, Berlin, 1990).
 - [19] S. Grabowski, K. Kadau, and P. Entel, *Phase Trans.* **75**, 265 (2002).
 - [20] H. Mehrer and R. Galler, *J. All. Comp.* **342**, 296 (2002).
 - [21] P.A. Kalugin and A. Katz, *Europhys. Lett.* **21**, 921 (1993).
 - [22] H. Mehrer and R. Galler, private communication.
 - [23] G. Kresse and J. Furthmüller, VASP – The Vienna Ab-initio Simulation Package,
<http://cms.mpi.univie.ac.at/vasp/>
 - [24] G. Kresse and D. Joubert, *Phys. Rev. B* **59**, 1758 (1999).
 - [25] M.S. Daw and M.I. Baskes, *Phys. Rev. B* **29**, 6443 (1984).